




Article

Effect of Regenerated Cellulose Fibers Derived from Black Oat on Functional Properties of PVA-Based Biocomposite Film

Naresh Shahi ¹, Gautam Joshi ² and Byungjin Min ^{2,*}

¹ Integrative Biosciences Ph.D. Program, Tuskegee University, Tuskegee, AL 36088, USA; nshahi1164@tuskegee.edu

² Department of Food and Nutritional Sciences, Tuskegee University, Tuskegee, AL 36088, USA; gjoshi7156@tuskegee.edu

* Correspondence: bmin@tuskegee.edu; Tel.: +1-334-727-8393

Received: 11 August 2020; Accepted: 10 September 2020; Published: 14 September 2020



Abstract: In this study, agricultural residue from black oat, a cover crop usually grown to improve soil nutrients between the periods of regular crop production, was used as a source of cellulose fibers. Concentrations of 1, 3, and 5 wt. % of regenerated cellulose (RC) fibers blended in poly(vinyl alcohol) (PVA) solution were used to prepare the reinforced composite films (CFs) by the solvent cast method. Compared to neat PVA film (control), the effects of RC addition on functional properties of CFs, such as water absorption, transparency, thermal stability, and mechanical property were investigated. All CFs with different RC concentrations exhibited improved mechanical property and thermal stability while the swelling property was decreased, and no significant changes were observed in the film transparency as compared with the control film. Among the CFs, films with 3% RC significantly decreased water vapor transmission rate, swelling, and soluble fraction ($p < 0.05$). In addition, Young's modulus and tensile strength were increased by 40 MPa and 3 MPa, respectively, while elongation at break was decreased by 4%, compared to the control film. The results indicate that RC from black oat might be feasible as potential bio fillers to improve film properties in a bio-based composite matrix.

Keywords: cellulose; PVA; cover crop; biopolymers; composite films

1. Introduction

In recent years, the mass production of synthetic plastics derived from petroleum has generated a significant quantity of non-biodegradable wastes that have ended up in landfills, and harmful chemicals generated during the disposal process have resulted in environmental pollution, as well as becoming a health concern. Thus, environmentally friendly materials such as bioplastics with improved functionalities such as barrier property, heat stability, and high mechanical property are in high demand [1–3]. Biodegradable polymers such as poly(vinyl alcohol) (PVA) could play an essential role in maintaining a healthy ecosystem [4,5]. The PVA is water-soluble and it has an excellent film-forming capability. The presence of hydroxyl groups in PVA forms a strong H-bond with other hydrophilic surfaces and thus develops a high strength composite films [6]. The PVA can be used in a wide range of applications such as hydrogel for the controlled release of drugs, membranes for chemical separation, composite electroactive hydrogel, and flexible sensor with cellulose [3,7–10]. However, the application of PVA as packaging material is limited due to hydrophilic nature of PVA which causes film swelling, poor moisture barrier and mechanical property [11]. To overcome these drawbacks of PVA-based composites, many researchers' works have been focused on improving properties such

as moisture absorption and mechanical properties of packaging materials. For instance, to improve functional properties of composite materials, the incorporation of nanomaterials such as graphene oxide, carbon nanotube, calcium carbonate nanoparticles, zinc oxide, and nanocellulose are used [12–17]. Among the reinforcing fillers, nano cellulose, typically found in two forms; cellulose nanofibers (CNFs) or cellulose nanocrystals (CNCs), are renewable and used for composite reinforcement [18]. The CNFs contain more amorphous regions in their molecular structure than CNCs; thus, it facilitates greater mechanical strength, flexibility, and optical clarity in composite films [19]. The plant-derived nanocellulose can be extracted from various sources, such as woods, cotton, forest products/byproducts, and agricultural residues [12,20,21]. Plant biomass, such as cover crop residues, can also be a good source of lignocellulose. Our previous study demonstrated that the cellulose content of black oat waste was around ~25% and showed high thermal stability [22].

Cellulose is not soluble in common solvents because inter- and intra-molecular hydrogen bonds and partially crystalline structures limit the applications. Various techniques have been studied to dissolve cellulose, and some solvents including ionic liquids, NaOH/urea, LiOH/urea, and ZnCl₂ solutions could be a facile route for cellulose dissolution [23–25]. Among the solvents, the NaOH/urea solution is considered as more suitable for cellulose dissolution because it is relatively safer, environmentally friendly, and cost-effective method [26]. The PVA/CNF reinforced films are transparent, light, flexible, biodegradable, and moldable. Thus, it makes them excellent candidates for the fabrication of biocomposite films for various applications which include packaging materials [6,11]. It is reported that 2,2,6,6-tetramethylpiperidinyloxy (TEMPO) oxidized CNFs derived from rice straw were well dispersed into the PVA matrix, resulting in high strength and heat-stable composite films without losing the transparency of composite films [11]. Another study found that PVA/nanocellulose biocomposite films improved barrier property, especially at a small amount (1–3%) of TEMPO-mediated nanocellulose isolated from wheat straw [27]. It is also reported that PVA/CNFs composite films (80% light transmittance) made by nanofibers from corn husks were highly visible, with improved tensile strength [28]. These methods have improved the barrier and mechanical properties of the composite films, but nanocellulose (CNFs/CNCs) was derived from traditional resources such as wheat straw, rice straw, and corn husks. The effect of regenerated cellulose fibers from cover crops (black oat) on composite films is rarely available in the literature. Moreover, the reinforcement effect of the fibers from different raw materials and isolation techniques influence the properties of PVA-composite films [11].

Therefore, this study aims to investigate how the functional properties of PVA-based films are affected by regenerated cellulose derived from black oat residues.

2. Materials and Methods

2.1. Materials and Reagents

Cellulose fibers previously extracted from black oat (*Avena strigose Schreb*) in our laboratory, which contain around 25% dry weight of cellulose, were used in this study, and the cellulose decomposition temperature was more than 370 °C [22]. Briefly, cellulose was extracted using a neutral and acid detergent solution, followed by alkaline hydrogen peroxide solution at pH 11.05 [29,30]. Polymers and chemicals used in this study such as poly(vinyl alcohol) (Mw 89,000–98,000, 99+% hydrolyzed), glycerol (100%), sodium hydroxide (NaOH) pellets, and 30% hydrogen peroxide (H₂O₂) containing stabilizer, as well as urea crystals, were purchased from Sigma-Aldrich Co., St. Louis, MO, USA.

2.2. Preparation of Regenerated Cellulose and PVA-Cellulose Composite Film

Cellulose isolated from black oat was dissolved in alkali/urea solution and regenerated in the acid coagulation bath. Regenerated cellulose (RC) was used as a reinforcing material, and PVA was chosen as the matrix. The composite blend was prepared with various RC concentrations in the PVA solution along with glycerol. The suspension of the polymer mixture was mechanically treated by employing a

low-frequency ultrasonic probe to enhance dispersion and interfacial adhesion bonding between RC and PVA.

One gram of black oat-cellulose was mixed in 100 mL alkali urea solution (NaOH/urea/H₂O). The weight ratio of the alkali urea solution was 7:12:81, and the solution containing cellulose was stored at −20 °C for 12 h [1]. The precooled mixture was vigorously stirred by a tissue homogenizer (Tissue master 125, Omni International, Kennesaw, GA, USA) for 5 min in an ice bath. The resultant solution was centrifuged at 3500 rpm for 5 min to separate the dissolved and undissolved cellulose. Dissolved cellulose was regenerated in a beaker containing a 5% H₂SO₄ solution at room temperature for 5 min. The regenerated cellulose (RC) was harvested with centrifugation at 5000 rpm for 5 min. The harvested RC was washed three times with deionized water. Washed RC was mixed at different weight ratios (*w/w*) with 0%, 1% (0.03 g), 3% (0.09 g), and 5% (0.15 g) into 3% PVA solution, and samples are described as PVA, PVA-RC1, PVA-RC3, and PVA-RC5, respectively. Approximately 13% of glycerol was also added as a plasticizer and crosslinker. The weight percentage of glycerol was based on PVA and PVA-RC weight. It is reported that glycerol could be used as a crosslinker with xanthan and other biopolymers including cellulose, and to develop electrospun gelatin-glycerol nano-fibrous mats for biomedical application [31,32]. However, cross-linking properties of the glycerol was not analyzed in this study. The composite mixture was further homogenized using a low frequency (20 kHz) ultrasonic processor (GE760, USA) equipped with 13 mm diameter titanium probe (Sonics and Materials Inc., Newtown, CT, USA) for 10 min at 70% amplitude. The gas bubbles in the composite blend (25 mL) were removed by using a centrifuge at 1000 rpm for 1 min, and the solution was gently poured into a polyethylene Petri dish (90 mm diameter), and dried at 30 °C for 24 h. Then, samples were transferred to an environmental chamber (Memmert GmbH+Co.KG, Schwabach, Germany) of the relative humidity of 55 ± 2% at 30 °C, for the next 24 h at least, and film was peeled off from the petri dish for further analysis. The film thickness was measured by a digital caliper (Thomas Scientific, Swedesboro, NJ, USA), and each value was expressed as an average of five representative spots measurements. The thickness of the films ranged from 110 to 130 μm.

2.3. Characterization of the Cellulose/PVA Film

2.3.1. Moisture Absorption and Water Vapor Transmission Rate (WVTR)

A drying oven (Quincy Lab Inc., Chicago, IL, USA) was used for drying composite films. The dried samples were placed in an environmental chamber at 55 ± 2% relative humidity at 25 °C for 12 h. The samples were taken out and weight using a precision balance, and moisture absorption was calculated by the following equation [11].

$$\text{Moisture absorption (\%)} = \frac{w_f - w_i}{w_i} \times 100$$

where w_f is the final weight, and w_i is the initial weight of samples.

Water vapor transmission rates (WVTR) of the PVA-cellulose films were conducted according to ASTM E96-95 standard method [33]. WVTR in permeability cups (Thwing-Albert instrument, West Berlin, NJ, USA) was carried out at 25 °C and 55 ± 2% relative humidity. Films were dried in an oven at 105 °C for 2 h before testing.

2.3.2. Swelling and Soluble Properties

The water absorption ability and solubility of the films were measured. The films were cut into a square shape of a 1 × 1 cm area. Before measurement, all the films were dried in an oven until a constant weight was obtained (w_i). The dried films were immersed into 20 mL of deionized water at 25 ± 2 °C

for 72 h, and then films were removed, wiped with tissue to remove surface water, and weighted (w_f). The swelling and soluble fraction of the films were calculated by the following equations [34].

$$\text{Swelling (\%)} = \frac{w_f - w_d}{w_d} \times 100$$

$$\text{Soluble fraction (\%)} = \frac{w_i - w_d}{w_i} \times 100$$

where w_i is the weight of the film after drying at 105 °C for 2 h (before immersing into the water), w_f represents the weight of the film after immersion in distilled water, w_d is for oven-dry weight after immersion in distilled water.

2.3.3. Film Transparency

A spectrophotometer DR 600 (Hach Company, Loveland, CO, USA) was used to measure the transmittance of the films. The transmittance spectra between 400 and 1000 nm were recorded in triplicate [11]. Rectangular shaped samples of 1 × 1.25 cm were prepared and placed into the spectrophotometer cuvette. An empty cuvette was used as blank.

2.3.4. Fourier Transform Infrared Spectroscopy (FTIR) Analysis

Attenuated total reflectance—Fourier transform infrared spectroscopy (ATR-FTIR), Nicolet, Nexus model 670/870 (Thermo Electron Corporation, Madison, WI, USA) was used to obtain spectra for the thin films at room temperature. The experiments were carried out in the range of 650–4000 cm^{-1} with the resolution 4 cm^{-1} , and total scans were 32 per sample.

2.3.5. Thermal Property

Thermal gravimetric analysis (TGA) of samples was carried out using TGA Q50 (TA Instruments, New Castle, DE, USA). About 15 mg of samples were placed on the platinum pan of a TA instrument. Samples were heated under a nitrogen atmosphere to prevent the thermo-oxidative degradation process, from 30 to 600 °C at the constant heating rate of 10 °C/min.

2.3.6. Mechanical Properties

Mechanical properties of the films, including Young's modulus, tensile strength, and elongation at break were measured using Texture analyzer TA-HD Plus (Stable Microsystem, Godalming, UK). The standard method was used for testing (ASTM D882-12). All samples were conditioned for 48 h at 55 ± 2% relative humidity and 30 °C in the environmental chamber. The tensile test was repeated five times for each sample.

2.4. Statistical Analysis

The origin Pro 16 (Version:93E, Origin Lab Co., New Castle, DE, USA) was used for analyzing the experimental data. The differences in sample groups on the properties of composite films and the control film were evaluated using analysis of variance (ANOVA) and t-test. Tukey's multiple range test further analyzed the differences amongst the mean values of the properties of the films at 95% confidence level. The measurements were replicated at least three times for each sample tested. The level of significance was defined at $p < 0.05$.

3. Results and Discussion

3.1. Preparation of Regenerated Cellulose and PVA-RC Composite Blend

The PVA-based film fabrication process from cellulose fibers was extracted from black oat, and the output of each step is presented in Figure 1. It can be observed that bulky RC fibers are well dispersed

in PVA solution after ultrasonication, indicating a homogeneous composite blend with a gel-like solution. The ultrasonication uses sound energy to create acoustic cavitation of air bubbles in a solution. On collapsing, the bubbles produce microjets and shockwaves, which disintegrate bulk materials into nanoparticles and disperse filler in the PVA matrix [35–37]. Ultrasonic irradiation attributes to homogeneous dispersion of cellulose fibers in polymer blend and also exhibited good compatibility of the PVA/nanocellulose due to the interaction of hydrogen bonds [28]. The obtained homogenized solution was used to fabricate the PVA-based composite films and characterized the different properties of the film, which are discussed in the following sections.

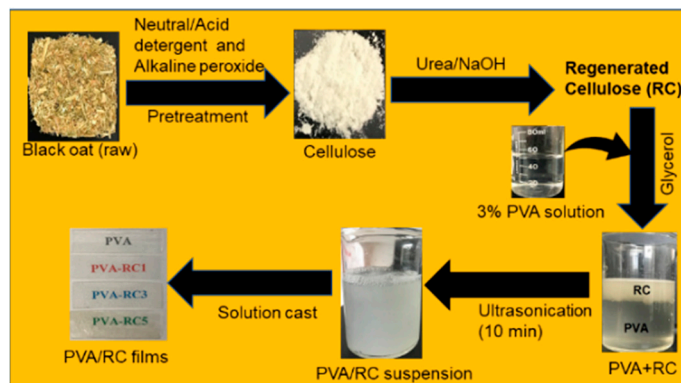


Figure 1. Flow diagram of isolation of regenerated cellulose (RC) derived from black oat and further application in poly(vinyl alcohol) (PVA) matrix with ultrasonication.

3.2. Moisture Absorbance and Water Vapor Transmission Rate (WVTR)

Among the film samples, the control PVA film showed the highest moisture absorption, which is around 8% (Supplementary Materials, Figure S1), as well as water vapor transmission rate ($\sim 3.0 \times 10^{-4} \text{ g/h}\cdot\text{m}^2$). Regardless of the samples, WVTR of the film is sharply increased at the beginning (first 4 h) then gradually increased or stagnant overtime, except in PVA-RC3 film, as shown in Figure 2. For example, WVTR for PVA-RC3 film after 12 h decreased by $\sim 30\%$. The decrease was attributed to increasing intermolecular bonding between RC fiber and PVA matrix. The water vapor transmission rate of neat PVA film was $\sim 2.47 \times 10^{-4} \text{ g/h}\cdot\text{m}^2$ and decreased significantly ($p < 0.05$) with the incorporation of RC. The WVTR of composite films is reduced with increasing RC concentration. As shown in Figure 2, among the concentrations of RC, 3% addition was the most effective in reducing WVTR in the film compared to 1% and 5% RC concentration ($p < 0.05$). The reduction in WVTR might be either an increase in crystallinity or due to reducing the free hydrophilic groups, thereby creating the tortuous path in composite films [38,39]. Additionally, the increase of WVTR might be due to the presence of agglomerates, which reduces the total surface area available for bonding, limiting the uniformity and compactness of the polymers [2]. Ultrasonication of PVA gel in less than 10 min decreased WVTR by 11%, and moisture resistance decreased around 12% of the resultant films was reported [40].

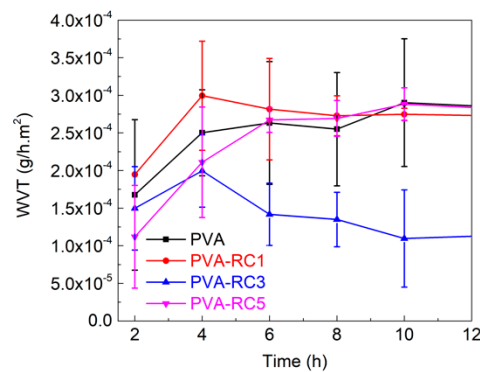


Figure 2. Water vapor transmission property of PVA and its composites.

3.3. Swelling and Soluble Fraction in Films

Figure 3a presents the values of the swelling percentage of PVA and PVA-RC composite films after being soaked in distilled water for 72 h. The PVA-RC composite films were less swollen than the neat PVA film, and the swelling percentage of composite films by water absorption is decreased with the addition of RC fibers. There was no significant difference in swelling percentage among neat PVA film, PVA-RC1, and PVA-RC5. However, the swelling percentage of PVA-RC3 film decreased by ~12%, compared to the control film (PVA). This result is consistent with the study on the PVA-cellulose composite film, with the addition of 5% rice straw CNFs, in which the water absorption of the films was decreased by ~11% [11]. Improved swelling properties of the composite films may be due to the interaction between RC fibers and PVA through the bonding of hydroxyl groups, thus decreasing the chance of water absorption [41]. Regardless of film compositions, there was a significant difference in soluble fraction of films between 60 h and 20 h ($p < 0.05$). Percent soluble fraction in film is decreased with the addition of regenerated cellulose (Figure 3b), but the difference was not significant compared to the control film.

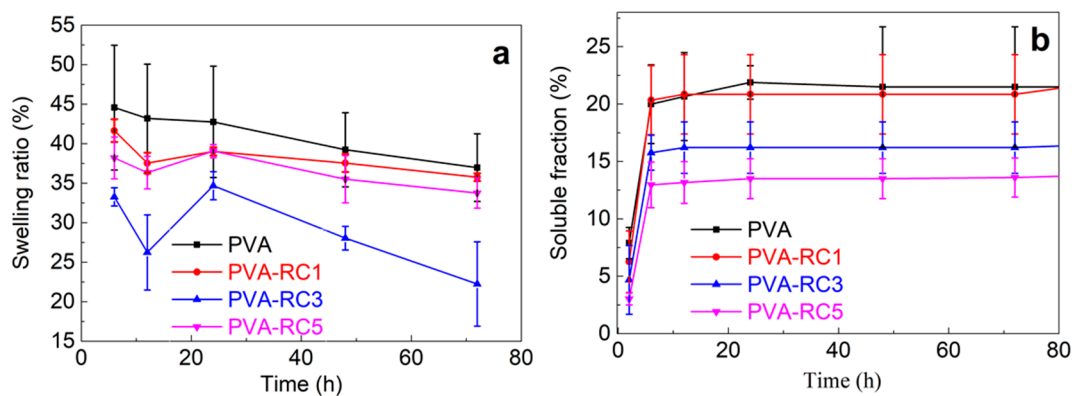


Figure 3. (a) Swelling and (b) Soluble fraction properties of neat PVA and composite films with different concentrations of RC load.

3.4. Transparency of the Films

The RC fiber dispersed throughout the film resulted in light scattering. Figure 4 (left) displays the transmittance spectrum of the neat PVA, and various composite films scanned between 400 to 1000 nm. The neat PVA film was the most transparent, and the films become less transparent with increased RC fiber content. For example, the transparency of PVA-RC5 film was the lowest among the films; it may be due to the presence of more cellulose fibers triggering more light scattering effect in films. In addition, there are few visible aggregates in PVA-RC5 films. Although decreased transparency of the PVA-RC5 is observed compared to other films, it was somewhat clear and transparent. As presented in Figure 4 (right), the label in the background of the films can be clearly seen through the films. Our results are

consistent with study results with rice straw CNFs/PVA composite films, in which the transparency of films was decreased with increasing cellulose concentration [11]. Another study also found similar results from PVA and bacterial cellulose composite films, in which films were less transparent with an increase in the bacterial cellulose nanofibers content [42].

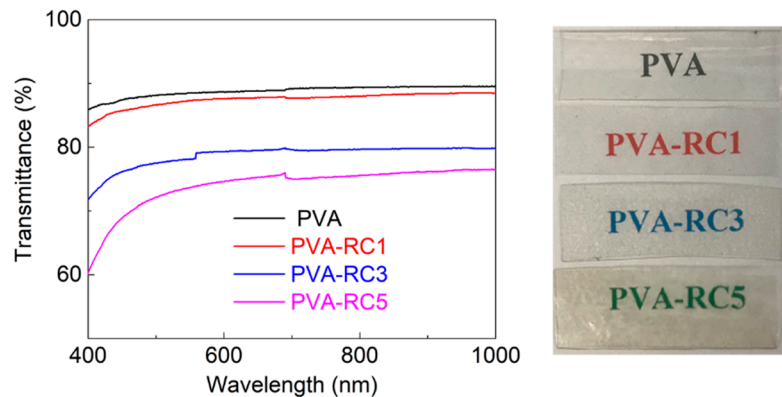


Figure 4. (Left) Transmittance spectrum of neat PVA and composite films with various RC fiber load and (Right) Images of neat PVA and composite films PVA, PVA-RC1, PVA-RC3, PVA-RC5 with 0%, 1%, 3%, and 5% RC fiber load, respectively.

3.5. Fourier Transform Infrared Spectroscopy (FTIR) Analysis

Figure 5 highlights the FTIR spectra of neat PVA and PVA-RC composite films with different weight compositions. From the FTIR spectra, the absorption band from $3500\text{--}3200\text{ cm}^{-1}$, 1089 cm^{-1} , and 1035 cm^{-1} can be observed for all samples originated from O-H stretching vibrations. These results indicate that composite films have excellent hydrophilicity. However, band intensity in this region is decreased with the addition of cellulose, indicating a decrease in hydrophilicity. This result also supports the swelling property in which the addition of fibers decreased in the swelling percentage of the composite films. It may be due to a lower number of free O-H groups in composite films than neat PVA films, which helps to form strong hydrogen bonds that lead to strengthening the composite film's mechanical properties. It is reported that the addition of bacterial cellulose nanofiber in a PVA matrix results in fewer O-H groups in the biocomposite films [42]. More importantly, the neat PVA film exhibited an obvious -OH stretching vibration peak around 3300 cm^{-1} (Figure 5a). As RC amount is increased, spectrum intensity is decreased, and the shift of the -OH group has occurred. In addition, a similar shift of -OH occurred from 1085 cm^{-1} (PVA) to 1089 cm^{-1} (PVA-RC), and from 915 cm^{-1} (PVA) to 913 cm^{-1} (PVA-RC), as presented in Figure 5b. These shifts indicate that the degree of free O-H decrease might have resulted from better dispersion of RC fibers in the PVA matrix and a subsequent increase in interfacial adhesive bonding [42]. The distinct peak around 2910 cm^{-1} and 1320 cm^{-1} is associated with C-H stretching, and this peak is also observed in all samples. The peaks associated with neat PVA films are as follows; 3276 cm^{-1} for stretching vibration of -OH groups, 2910 cm^{-1} for -CH₂ groups stretching, and 1417 cm^{-1} and 1320 cm^{-1} for C-H wagging and bending, respectively, and a sharp peak at $\sim 1140\text{ cm}^{-1}$ for the crystalline domain of the PVA [28,43]. The sharp crystalline peak may be due to the ultrasonication of the composite blend.

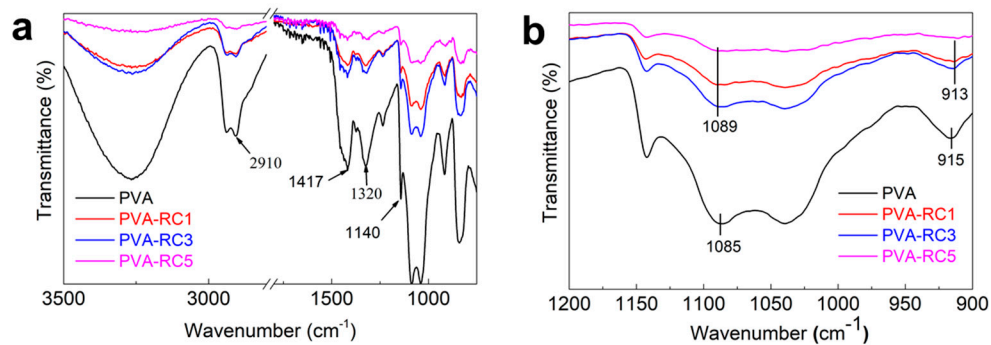


Figure 5. (a) Fourier Transform Infrared (FTIR) spectra of neat PVA and composite films with different concentrations of RC loadand (b) Magnified spectra indicate -OH group shift.

3.6. Thermal Gravimetric Analysis (TGA)

The thermal stability of the films was evaluated with a TGA measurement, and the derivative thermogravimetry (DTG) profiles are presented in Figure 6a, and Figure 6b, respectively. Initially, the weight of the films slightly decreased due to the evaporation of absorbed water (50–120 °C), which corresponded to peak (i) in the DTG graph. The second major weight change occurred in the temperature range 200 to 350 °C, the major weight losses observed in this region, which was attributed to the degradation of the side chain of PVA, and thermal degradation of the RC fibers, which corresponds to peaks (ii and iii) in the DTG graph [28]. In this step, the decomposition temperature of PVA and PVA-RC1 decreased as compared with PVA-RC3 and PVA-RC5; two maximum temperatures in this region are around 270 and 360 °C [44]. The third degradation region corresponding to peak (iv) was observed around 400 to 500 °C, which was attributed to the decomposition of the main PVA chain, and the maximum decomposition temperature of this region is approximately 350 °C [44,45]. The maximum thermal decomposition temperature (T_{max}) of the composite films increased, except in PVA-RC1, which indicates that the thermal stability of film increased with the addition of RC fibers compared to PVA film (control). The elevation of decomposition temperature in the composite films may be due to an increased crystallinity after ultrasonication. The ultrasonication increased the PVA crystallinity index of the films and compatibility of the polymer chain structure [40]. Our results are similar to PVA-crystalline and PVA-nano cellulose composite film, in which the degradation process of the composite films was slightly higher than that of pure PVA films [7,28]. The detailed weight loss data of each film with increasing temperature is available in the Supplementary Materials (Table S1).

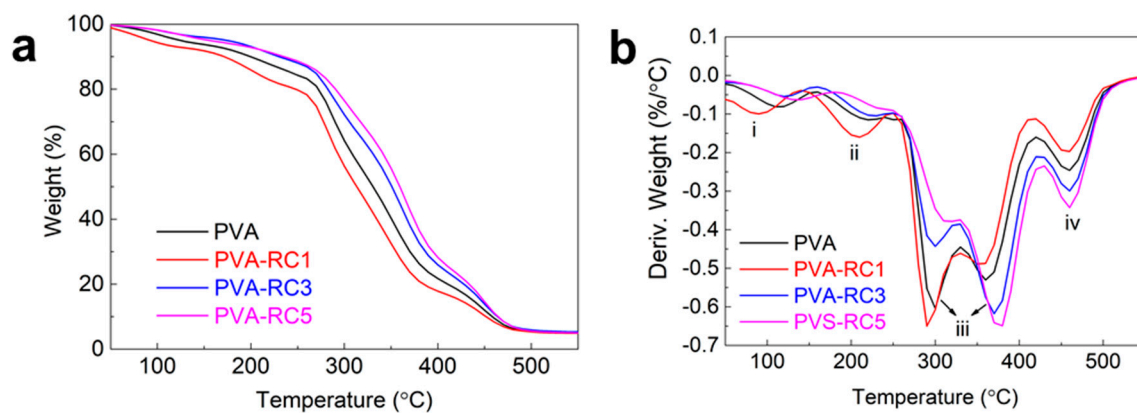


Figure 6. (a) Thermal gravimetric analysis (TGA) and (b) Derivative thermogravimetry (DTG) profiles of neat PVA and its composite film.

3.7. Mechanical Properties of PVA Composite Films

The stress-strain graph for neat PVA and PVA-RC composite films is displayed in Figure 7 and Table 1 present the data corresponding to Young's modulus, tensile strength, and percentage elongation at break. It was observed that a small decrease in the tensile strength of composite films with PVA-RC5 compared to control PVA film, while there was an increase in tensile strength in PVA-RC3. The tensile strength is increased by ~2 MPa with a 3% loading of RC compared to the control film, and there was no significant difference in tensile strength. Another study was conducted on PVA-bacterial cellulose composite films, in which the tensile strength of the composite films was increased from 27.3 to 33.9 MPa after the addition of 2.5 mL of bacterial cellulose fiber in PVA matrix [42]. A similar result was also reported that the tensile strength of the PVA-CNFs composite film was improved at 3% addition of rice straw CNFs [11]. It is thought that excessive amount of filler materials over a certain percentage triggers agglomeration so that it weakens tensile strength of films [46]. The Young's modulus of the PVA-RC composite films was higher than the neat PVA, as presented in Table 1. The increased Young's modulus after the addition of RC fibers is attributed to the presence of disintegrated RC, creating interface hydrogen bonds with the PVA matrix, thus anchoring the PVA chains against the movement.

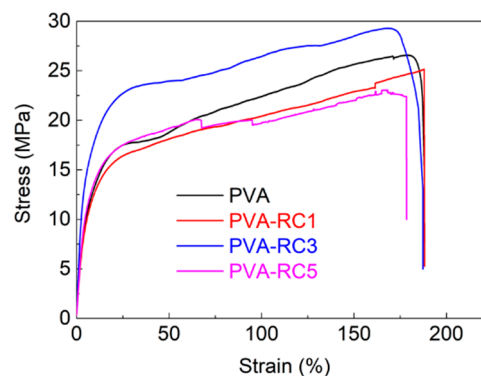


Figure 7. Stress-strain curve of neat PVA and composite films with different concentrations of RC load.

Table 1. Mechanical properties of PVA and its composite films.

Sample	Young's Modulus (MPa)	Tensile Strength (MPa)	Elongation at Break (%)
PVA	70 ± 10	25 ± 2	170 ± 29
PVA-RC1	73 ± 10	24 ± 2	177 ± 23
PVA-RC3	110 ± 20	27 ± 3	165 ± 25
PVA-RC5	112 ± 10	17 ± 3	155 ± 16

Different from the tensile strength results, the elongation at break exhibited a declining pattern, with increasing RC fiber from 1% to 5% in PVA-RC composite films. The elongation at break (177%) of the composite film was the highest at 1% RC, but it was decreased with the gradual addition of RC. Similar changes in the elongation at break of PVA composite films were also reported by many researchers [11,28,42,47]. For example, the tensile strength and strain at break of the PVA/CNFs films increased by 1.47 and 1.87 times, respectively, with 1% nanofibrillated cellulose isolated from corn husk compared to PVA but decreased with over 1% content [28]. It is reported that a similar effect in biocomposite films in which elongation at break of neat PVA films and composite films was 171% and 164%, respectively [42]. The stiff network structure of cellulose fibers limits the chain mobility of PVA molecules in the composite decreased in the elongation property of the composite films [11].

4. Conclusions

This article reports a facile and efficient method of fabricating PVA-based composite films reinforced with regenerated cellulose (RC) derived from black oat. To obtain a homogeneous mixture of a composite blend of RC and PVA, the solution of the composite mixture was ultrasonically irradiated. Our result showed that 3% of RC addition into PVA matrix is optimal for the superior quality of composite films among the tested films. The fabrication of PVA-based biocomposite films reinforced with RC showed high-quality composite films with improved moisture barrier property, decreased swelling behavior, and improved heat resistance property. However, the differences in tensile strength between PVA-based RC composite films and PVA film alone were not significant. From the results, it is thought that cover crops like black oat might be a feasible source for bio-based packaging materials.

Supplementary Materials: The following are available online at <http://www.mdpi.com/2227-9717/8/9/1149/s1>, Figure S1: Moisture absorption (%) of neat PVA and composite films in 24 h and Table S1: Remaining weight (%) of neat PVA and composite films with increasing temperature.

Author Contributions: N.S. designed and performed the experiments, analyzed the data, and prepared the original manuscript. B.M. conceived the study, reviewed, edited the manuscript, and supervised the research. G.J. supported to perform the experiments. All authors have read and agreed to the published version of the manuscript.

Funding: This research was funded by the United States Department of Agriculture (USDA)/National Institute of Food and Agriculture (NIFA) (grant # 2015-38821-24376) and the USDA Evans Allen project.

Conflicts of Interest: The authors declare no conflict of interest.

References

1. Yang, Q.; Fukuzumi, H.; Saito, T.; Isogai, A.; Zhang, L. Transparent Cellulose Films with High Gas Barrier Properties Fabricated from Aqueous Alkali/Urea Solutions. *Biomacromolecules* **2011**, *12*, 2766–2771. [[CrossRef](#)] [[PubMed](#)]
2. Shanmugam, K.; Doosthosseini, H.; Varanasi, S.; Garnier, G.; Batchelor, W. Nanocellulose films as air and water vapour barriers: A recyclable and biodegradable alternative to polyolefin packaging. *Sustain. Mater. Technol.* **2019**, *22*, e00115. [[CrossRef](#)]
3. Christophliemk, H.; Johansson, C.; Ullsten, H.; Järnström, L. Oxygen and water vapor transmission rates of starch-poly(vinyl alcohol) barrier coatings for flexible packaging paper. *Prog. Org. Coat.* **2017**, *113*, 218–224. [[CrossRef](#)]
4. Abdulkhani, A.; Marvast, E.H.; Ashori, A.; Hamzeh, Y.; Karimi, A.N. Preparation of cellulose/polyvinyl alcohol biocomposite films using 1-n-butyl-3-methylimidazolium chloride. *Int. J. Boil. Macromol.* **2013**, *62*, 379–386. [[CrossRef](#)]
5. Asad, M.; Saba, N.; Asiri, A.M.; Jawaid, M.; Indarti, E.; Wanrosli, W. Preparation and characterization of nanocomposite films from oil palm pulp nanocellulose/poly (Vinyl alcohol) by casting method. *Carbohydr. Polym.* **2018**, *191*, 103–111. [[CrossRef](#)]
6. Wang, B.; Li, D. Strong and optically transparent biocomposites reinforced with cellulose nanofibers isolated from peanut shell. *Compos. Part A Appl. Sci. Manuf.* **2015**, *79*, 1–7. [[CrossRef](#)]
7. Li, W.; Yue, J.; Liu, S. Preparation of nanocrystalline cellulose via ultrasound and its reinforcement capability for poly(vinyl alcohol) composites. *Ultrason. SonoChem.* **2012**, *19*, 479–485. [[CrossRef](#)]
8. Chen, C.; Xu, Z.; Ma, Y.; Liu, J.; Zhang, Q.; Tang, Z.; Fu, K.; Yang, F.; Xie, J. Properties, vapour-phase antimicrobial and antioxidant activities of active poly(vinyl alcohol) packaging films incorporated with clove oil. *Food Control.* **2018**, *88*, 105–112. [[CrossRef](#)]
9. Sekertekin, Y.; Bozyel, I.; Gokcen, D. A Flexible and Low-Cost Tactile Sensor Produced by Screen Printing of Carbon Black/PVA Composite on Cellulose Paper. *Sensors* **2020**, *20*, 2908. [[CrossRef](#)]
10. Jayaramudu, T.; Ko, H.-U.; Kim, H.C.; Kim, J.W.; Muthoka, R.M.; Kim, J. Electroactive Hydrogels Made with Polyvinyl Alcohol/Cellulose Nanocrystals. *Materials* **2018**, *11*, 1615. [[CrossRef](#)]
11. Wang, Z.; Qiao, X.; Sun, K. Rice straw cellulose nanofibrils reinforced poly(vinyl alcohol) composite films. *Carbohydr. Polym.* **2018**, *197*, 442–450. [[CrossRef](#)] [[PubMed](#)]

12. Dungani, R.; H.P.S., A.K.; Aprilia, N.A.S.; Sumardi, I.; Aditiawati, P.; Darwis, A.; Karliati, T.; Sulaeman, A.; Rosamah, E.; Riza, M. Bionanomaterial from agricultural waste and its application. *Cellul.-Reinf. Nanofibre Compos.* **2017**, *45*–88. [[CrossRef](#)]
13. Ng, H.-M.; Sin, L.T.; Tee, T.-T.; Bee, S.-T.; Hui, D.; Low, C.-Y.; Rahmat, A. Extraction of cellulose nanocrystals from plant sources for application as reinforcing agent in polymers. *Compos. Part B Eng.* **2015**, *75*, 176–200. [[CrossRef](#)]
14. Siepmann, J.; Siegel, R.A.; Rathbone, M.J. *Fundamentals and Applications of Controlled Release Drug Delivery*; Springer: New York, NY, USA, 2012; pp. 1–594. [[CrossRef](#)]
15. Asim, N.; Emdadi, Z.; Mohammad, M.; Yarmo, M.; Sopian, K. Agricultural solid wastes for green desiccant applications: An overview of research achievements, opportunities and perspectives. *J. Clean. Prod.* **2015**, *91*, 26–35. [[CrossRef](#)]
16. Mandal, A.; Chakrabarty, D. Isolation of nanocellulose from waste sugarcane bagasse (SCB) and its characterization. *Carbohydr. Polym.* **2011**, *86*, 1291–1299. [[CrossRef](#)]
17. Kauldhar, B.S.; Yadav, S.K. Turning waste to wealth: A direct process for recovery of nano-silica and lignin from paddy straw agro-waste. *J. Clean. Prod.* **2018**, *194*, 158–166. [[CrossRef](#)]
18. Salas, C.; Nypelö, T.; Rodríguez-Abreu, C.; Carrillo, C.; Rojas, O.J. Nanocellulose properties and applications in colloids and interfaces. *Curr. Opin. Colloid Interface Sci.* **2014**, *19*, 383–396. [[CrossRef](#)]
19. Xu, X.; Liu, F.; Jiang, L.; Zhu, J.Y.; Haagensohn, D.; Wiesenborn, D.P. Cellulose Nanocrystals vs. Cellulose Nanofibrils: A Comparative Study on Their Microstructures and Effects as Polymer Reinforcing Agents. *ACS Appl. Mater. Interfaces* **2013**, *5*, 2999–3009. [[CrossRef](#)]
20. Yahya, M.A.; Al-Qodah, Z.; Ngah, C.Z. Agricultural bio-waste materials as potential sustainable precursors used for activated carbon production: A review. *Renew. Sustain. Energy Rev.* **2015**, *46*, 218–235. [[CrossRef](#)]
21. Ajao, O.A.; Marinova, M.; Savadogo, O.; Paris, J. Hemicellulose based integrated forest biorefineries: Implementation strategies. *Ind. Crop. Prod.* **2018**, *126*, 250–260. [[CrossRef](#)]
22. Shahi, N.; Joshi, G.; Min, B. Potential Sustainable Biomaterials Derived from Cover Crops. *BioResources* **2020**, *15*, 5641–5652. [[CrossRef](#)]
23. Endo, T.; Aung, E.M.; Fujii, S.; Hosomi, S.; Kimizu, M.; Ninomiya, K.; Takahashi, K. Investigation of accessibility and reactivity of cellulose pretreated by ionic liquid at high loading. *Carbohydr. Polym.* **2017**, *176*, 365–373. [[CrossRef](#)] [[PubMed](#)]
24. Klemm, D.; Philipp, B.; Heinze, T.; Heinze, U.; Wagenknecht, W. *Comprehensive Cellulose Chemistry*; Wiley: Hoboken, NJ, USA, 1998.
25. Zhao, G.; Lyu, X.; Lee, J.; Cui, X.; Chen, W.N. Biodegradable and transparent cellulose film prepared eco-friendly from durian rind for packaging application. *Food Pack. Shelf Life* **2019**, *21*, 100345. [[CrossRef](#)]
26. Cai, J.; Zhang, L.; Zhou, J.; Li, H.; Chen, H.; Jin, H. Novel Fibers Prepared from Cellulose in NaOH/Urea Aqueous Solution. *Macromol. Rapid Commun.* **2004**, *25*, 1558–1562. [[CrossRef](#)]
27. Espinosa, E.; Bascón-Villegas, I.; Rosal, A.; Pérez-Rodríguez, F.; Chinga-Carrasco, G.; Rodríguez, A. PVA/(ligno)nanocellulose biocomposite films. Effect of residual lignin content on structural, mechanical, barrier and antioxidant properties. *Int. J. Boil. Macromol.* **2019**, *141*, 197–206. [[CrossRef](#)]
28. Xiao, S.; Gao, R.; Gao, L.; Li, J. Poly(vinyl alcohol) films reinforced with nanofibrillated cellulose (NFC) isolated from corn husk by high intensity ultrasonication. *Carbohydr. Polym.* **2016**, *136*, 1027–1034. [[CrossRef](#)]
29. Godin, B.; Agneessens, R.; Gerin, P.A.; Delcarte, J. Composition of structural carbohydrates in biomass: Precision of a liquid chromatography method using a neutral detergent extraction and a charged aerosol detector. *Talanta* **2011**, *85*, 2014–2026. [[CrossRef](#)]
30. Shahi, N.; Min, B.; Sapkota, B.; Rangari, V.K. Eco-Friendly Cellulose Nanofiber Extraction from Sugarcane Bagasse and Film Fabrication. *Sustainability* **2020**, *12*, 6015. [[CrossRef](#)]
31. Bilanovic, D.; Starosvetsky, J.; Armon, R. Cross-linking xanthan and other compounds with glycerol. *Food Hydrocoll.* **2015**, *44*, 129–135. [[CrossRef](#)]
32. Morsy, R.; Hosny, M.; Reicha, F.; Elnimr, T.; Reisha, F. Developing and physicochemical evaluation of cross-linked electrospun gelatin–glycerol nanofibrous membranes for medical applications. *J. Mol. Struct.* **2017**, *1135*, 222–227. [[CrossRef](#)]
33. C16 Committee Test Methods for Water Vapor Transmission of Materials. *ASTM Int.* **2016**. [[CrossRef](#)]

34. Lee, H.; You, J.; Jin, H.-J.; Kwak, H.W. Chemical and physical reinforcement behavior of dialdehyde nanocellulose in PVA composite film: A comparison of nanofiber and nanocrystal. *Carbohydr. Polym.* **2020**, *232*, 115771. [[CrossRef](#)] [[PubMed](#)]
35. Bang, J.H.; Suslick, K.S. Applications of Ultrasound to the Synthesis of Nanostructured Materials. *Adv. Mater.* **2010**, *22*, 1039–1059. [[CrossRef](#)] [[PubMed](#)]
36. Li, J.; Wei, X.; Wang, Q.; Chen, J.; Chang, G.; Kong, L.; Su, J.; Liu, Y. Homogeneous isolation of nanocellulose from sugarcane bagasse by high pressure homogenization. *Carbohydr. Polym.* **2012**, *90*, 1609–1613. [[CrossRef](#)] [[PubMed](#)]
37. Zhou, G.-D.; Zhu, H.; Phillips, T.D.; Wang, J.; Wang, S.-Z.; Wang, F.; Amendt, B.A.; Couroucli, X.I.; Donnelly, K.C.; Moorthy, B. Effects of Dietary Fish Oil on the Depletion of Carcinogenic PAH-DNA Adduct Levels in the Liver of B6C3F1 Mouse. *PLoS ONE* **2011**, *6*, e26589. [[CrossRef](#)]
38. John, M.J.; Thomas, S. Biofibres and biocomposites. *Carbohydr. Polym.* **2008**, *71*, 343–364. [[CrossRef](#)]
39. Shankar, S.; Wang, L.-F.; Rhim, J.-W. Effect of melanin nanoparticles on the mechanical, water vapor barrier, and antioxidant properties of gelatin-based films for food packaging application. *Food Pack. Shelf Life* **2019**, *21*, 100363. [[CrossRef](#)]
40. Abrial, H.; Atmajaya, A.; Mahardika, M.; Hafizulhaq, F.; Kadriadi; Handayani, D.; Sapuan, S.; Ilyas, R. Effect of ultrasonication duration of polyvinyl alcohol (PVA) gel on characterizations of PVA film. *J. Mater. Res. Technol.* **2020**, *9*, 2477–2486. [[CrossRef](#)]
41. Bai, H.; Li, Z.; Zhang, S.; Wang, W.; Dong, W. Interpenetrating polymer networks in polyvinyl alcohol/cellulose nanocrystals hydrogels to develop absorbent materials. *Carbohydr. Polym.* **2018**, *200*, 468–476. [[CrossRef](#)]
42. Abrial, H.; Kadriadi; Mahardika, M.; Handayani, D.; Sugiarti, E.; Muslimin, A.N. Characterization of disintegrated bacterial cellulose nanofibers/PVA bionanocomposites prepared via ultrasonication. *Int. J. Boil. Macromol.* **2019**, *135*, 591–599. [[CrossRef](#)]
43. Sun, X.; Lu, C.; Liu, Y.; Zhang, W.; Zhang, X. Melt-processed poly(vinyl alcohol) composites filled with microcrystalline cellulose from waste cotton fabrics. *Carbohydr. Polym.* **2014**, *101*, 642–649. [[CrossRef](#)] [[PubMed](#)]
44. Gong, X.; Tang, C.-Y.; Pan, L.; Hao, Z.; Tsui, C.P. Characterization of poly(vinyl alcohol) (PVA)/ZnO nanocomposites prepared by a one-pot method. *Compos. Part B Eng.* **2014**, *60*, 144–149. [[CrossRef](#)]
45. Liu, D.; Sun, X.; Tian, H.; Maiti, S.; Ma, Z. Effects of cellulose nanofibrils on the structure and properties on PVA nanocomposites. *Cellulose* **2013**, *20*, 2981–2989. [[CrossRef](#)]
46. Robles, E.; Urruzola, I.; Labidi, J.; Serrano, L. Surface-modified nano-cellulose as reinforcement in poly(lactic acid) to conform new composites. *Ind. Crop. Prod.* **2015**, *71*, 44–53. [[CrossRef](#)]
47. Choo, K.; Ching, Y.C.; Chuah, C.H.; Julai, S.; Liou, N.-S. Preparation and Characterization of Polyvinyl Alcohol-Chitosan Composite Films Reinforced with Cellulose Nanofiber. *Materials* **2016**, *9*, 644. [[CrossRef](#)]

